Widely tunable single-bandpass microwave photonic filter based on polarization processing of a nonsliced broadband optical source

Hui Wang, Jian Yu Zheng, Wei Li, Li Xian Wang, Ming Li, Liang Xie,* and Ning Hua Zhu

State Key Laboratory on Integrated Optoelectronics, Institute of Semiconductors, Chinese Academy of Sciences, Beijing 100083, China
**Corresponding author: xiel@semi.ac.cn*

Received July 23, 2013; revised September 26, 2013; accepted October 15, 2013;
posted October 16, 2013 (Doc. ID 194401); published November 14, 2013

We propose a new scheme of microwave photonic filter (MPF) based on the polarization processing of a broadband optical source (BOS), which features single-bandpass response and a wide span of operation bandwidth. The BOS is orthogonally polarized by a polarization division multiplexing emulator (PDME) with a tunable time delay between the two polarization states and incident at ±45° to one principle axis of a polarization modulator (PolM). The PDME cascades a PolM, and a polarizer realizes a microwave modulation making the phase of the carrier able to be tuned while ±1st sidebands remain unchanged, which after propagating in a dispersive medium results in a tunable single-bandpass response in the RF domain. We experimentally verify the MPF. By adjusting the time delay and the optical spectrum bandwidth, the passband center frequency is continuously tuned from DC to 20 GHz and the 3 dB passband bandwidth changes while the optical spectrum bandwidth ranges from 1 to 4 nm.

OCIS codes: (060.5625) Radio frequency photonics; (060.2420) Fibers, polarization-maintaining; (060.4510) Optical communications; (070.2615) Frequency filtering.
http://dx.doi.org/10.1364/OL.38.004857

Microwave photonic filtering technology plays an important role in the field of high-speed radio frequency and microwave signal processing, thanks to the distinct features such as low power loss, large operation bandwidth, high reconfigurability, and immunity to electromagnetic interference [1–3]. Since the microwave photonic filter (MPF) is a typical microwave photonic signal processing system, different kinds of MPFs have been widely investigated in the last two decades. However, these MPFs mainly have the discrete time finite impulse response (FIR) that would result in a periodic response in the frequency domain [4–9]. Recently, a single-bandpass MPF based on a dual-input Mach–Zehnder modulator (MZM) and RF decay effect was reported [10], which was complicated with the use of liquid crystal on silicon (LCoS) pixels and the carrier suppression effect (CSE) severely limited the frequency tunability. To avoid using the LCoS pixels, Xue *et al.* reported a single-bandpass MPF using a nonsliced broadband optical source (BOS) and variable optical carrier time shift method [11]. However, adjusting and maintaining the light waves' polarization directions in each arm made the MPF complicated in practical applications and susceptible to the environmental perturbations. Reference [12] presented another simple structure of a dual-input MZM with unbalanced input fiber lengths from the BOS into the two arms of the modulator, which may suffer from a bias drifting problem. The MPFs based on polarization modulation, which feature wideband operation, high tuning speed, and compact structure [13], have attracted more and more attention in recent years. So far, however, these MPFs are just limited to having a periodic frequency response.

In this Letter, we demonstrate a novel structure of MPF based on polarization division multiplexing and polarization modulation technology. Thanks to the compact elements of the polarization division multiplexing emulator (PDME) and polarization modulator (PolM), the polarization-dependent light waves can be processed, respectively, combined orthogonally, and then modulated simultaneously. The proposed MPF can operate steadily by featuring a single bandpass with baseband suppression and a wide tuning range without the problem of the CSE. By adjusting the time delay in the PDME and the bandwidth of the BOS, the proposed MPF experimentally demonstrates not only a large span of operation bandwidth without significant variation to the shape of the frequency response but also a continuously tunable 3 dB passband bandwidth.

The main part of our scheme and the operation principle is shown in Fig. 1. The BOS is first filtered from an amplified spontaneous emission (ASE) source by an inner tunable bandpass filter (TBPF) with a rectangle-like filtering window and then polarized by a polarizer (Pol.1). The PDME is a compact device, which internally

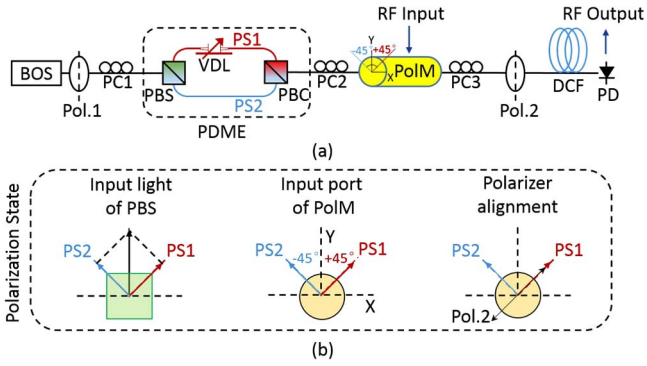

Fig. 1. (a) Experimental setup. (b) Polarization alignment. Broadband optical source (BOS), polarization controller (PC), polarization division multiplexing emulator (PDME), polarization beam splitter (PBS), polarization beam combiner (PBC), variable delay line (VDL), polarization modulator (PolM), polarizer (Pol), dispersion compensating fiber (DCF), and photodiode (PD).

consists of a polarization beam splitter (PBS), a polarization beam combiner (PBC), and a variable delay line (VDL) in one polarization channel. A polarization controller (PC1) is used to balance the intensity of the two light waves split by the PBS; the VDL introduces a tunable time delay between two polarized states (PS1 and PS2). At the output of the PBC, two polarized light waves are combined orthogonally into one single-mode fiber and aligned at ±45° to the principle y axis of the PolM by the PC2, as shown in Fig. 1(b). The PolM is a two-orthogonal-channel phase modulator, which can modulate the optical phase simultaneously along the two principle axes with opposite modulation indices over a RF bandwidth of 40 GHz. Assuming a cosine modulation, a signal of $V_m \cos(\omega_m t)$ is imposed to the PolM, where V_m is the modulation amplitude, ω_m is the modulation frequency, and we define the input BOS as $E(t)$, the output of the PolM is

$$E_{\mathrm{PolM}}(t) = \begin{bmatrix} E_x \\ E_y \end{bmatrix} \propto \begin{bmatrix} E(t)e^{j(\beta\cos(\omega_m t))} \\ E(t)e^{j(-\beta\cos(\omega_m t)+\varphi_0)} \end{bmatrix}, \quad (1)$$

where β is the phase modulation index of the PolM expressed in radians as $\beta = \pi V_m/V_\pi$, V_π is the half-wave voltage of the PolM, and φ_0 is the static phase difference induced by PC2 between E_x and E_y. Following, a polarizer oriented with the same polarization of the PS1 allows the PS1 to pass through while orthogonally blocking the PS2. The output optical field from the Pol.2 is defined as $E_{\mathrm{Pol.2}}(t)$, and each optical component of $E_{\mathrm{Pol.2}}(t)$ from the two modulated polarization states is considered as $E_{\mathrm{PS1}}(t)$ and $E_{\mathrm{PS2}}(t)$. The $E_{\mathrm{Pol.2}}(t)$ can then be expressed as

$$\begin{aligned} E_{\mathrm{Pol.2}}(t) &= E_{\mathrm{PS1}}(t) + E_{\mathrm{PS2}}(t) \\ &\propto E(t)\left\{\cos\left[\beta\cos(\omega_m t) - \frac{\varphi_0}{2}\right]\right. \\ &\quad \left. + j\sin\left[\beta\cos(\omega_m t) - \frac{\varphi_0}{2}\right]\right\}. \end{aligned} \quad (2)$$

If $\varphi_0 = 0$, then by applying the Jacobi–Anger expansion to Eq. (2), we have

$$\begin{aligned} E_{\mathrm{Pol.2}}(t) &= E_{\mathrm{PS1}}(t) + E_{\mathrm{PS2}}(t) \\ &\propto E(t)\{\cos[\beta\cos(\omega_m t)] + j\sin[\beta\cos(\omega_m t)]\} \\ &= E(t)\begin{Bmatrix} J_0(\beta) + 2\sum_{n=1}^{\infty}(-1)^n J_{2n}(\beta)\cos(2n\omega_m t) \\ -2j\sum_{n=1}^{\infty}(-1)^n J_{2n-1}(\beta)\cos[(2n-1)\omega_m t] \end{Bmatrix}. \end{aligned} \quad (3)$$

Under a small-signal modulation condition, Eq. (3) can be simplified as

$$\begin{aligned} E_{\mathrm{Pol.2}}(t) &= E_{\mathrm{PS1}}(t) + E_{\mathrm{PS2}}(t) \\ &\approx J_0(\beta)E(t) + j2J_1(\beta)E(t)\cos(\omega_m t). \end{aligned} \quad (4)$$

It is worth noting that the optical carrier and sidebands in Eq. (4) derive from the BOS in different polarization states, i.e., the PS1 and PS2 as shown in Fig. 1(b). If a time delay $\Delta\tau$ is introduced between the two orthogonal polarization states, Eq. (4) can be rewritten as

$$\begin{aligned} E_{\mathrm{Pol.2}}(t) &= E_{\mathrm{PS1}}(t)|_{t-\Delta\tau} + E_{\mathrm{PS2}}(t) = E_{\mathrm{PS1}}(t-\Delta\tau) + E_{\mathrm{PS2}}(t) \\ &\propto J_0(\beta)E(t-\Delta\tau) + j2J_1(\beta)E(t)\cos(\omega_m t), \end{aligned} \quad (5)$$

where $J_n(n = 0, 1)$ is the Bessel function of the first kind of order n. Here if we assume the time delay difference induced into the $E_{\mathrm{PS1}}(t)$ by the VDL is $\Delta\tau$, then the $E_{\mathrm{PS1}}(t)$ is changed into $E_{\mathrm{PS1}}(t-\Delta\tau)$ and the Fourier transform of Eq. (5) is given as

$$\begin{aligned} E_{\mathrm{Pol.2}}(\Omega) &\propto J_0(\beta)E(\Omega)e^{-j\Omega\Delta\tau} \\ &\quad + jJ_1(\beta)[E(\Omega-\omega_m) + E(\Omega+\omega_m)]. \end{aligned} \quad (6)$$

This means we can consider $E_{\mathrm{PS1}}(\Omega)$ as an optical carrier and the corresponding $\Omega \pm \omega_m$ components of $E_{\mathrm{PS2}}(\Omega)$ as ±1st sidebands under carrier-suppressed intensity modulation. Combining the two parts together shows that along the optical frequency axis, the phases of the optical carriers continuously change while the phases of the sidebands stay the same. As shown in Fig. 2, the angle of φ varies periodically, which results in a continuous alternation between intensity modulation and phase modulation; thus, if detected by a photodiode, a sinusoidal electrical slicing effect can be induced. Because the carrier phase periodicity is determined by the time delay of $\Delta\tau$, the electrical slicing response can be continuously tuned by adjusting the VDL in the PDME. It is worth noting that the operational principle of our scheme is different from that in [11]. In [11], the BOS is split into two paths with one path time-delayed and modulated by an intensity modulator to perform carrier suppressed double-sideband modulation. In our scheme, however, the BOS in both orthogonal polarizations is polarization modulated by the PolM. For both polarizations, the odd and even order-modulated components derive from the BOS in different polarizations thanks to the polarization modulation. Therefore, if we impose a time delay on the BOS in the orthogonal polarizations, this delay amount can be introduced between the odd and even order-modulated components.

Following, a dispersion compensating fiber (DCF) then works as a dispersion medium to map the modulated optical spectrum into the time domain. The frequency-dependent dispersion caused by the DCF can be expressed as

$$\Phi(\Omega) = e^{-j\theta_2\frac{(\Omega-\Omega_0)^2}{2}}, \quad (7)$$

where θ_2 is the total dispersion and Ω_0 is the reference frequency of the BOS. With the dispersive effect, the output optical field of the DCF is $E_{\mathrm{out}}(\Omega) = E_{\mathrm{Pol.2}}(\Omega)$, $\Phi(\Omega)$.

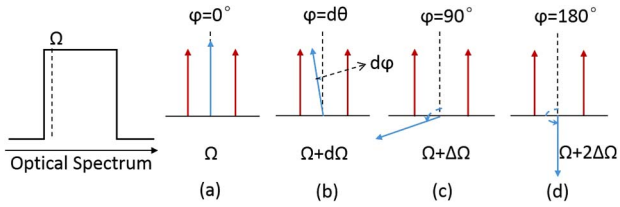

Fig. 2. Phase evolution of optical carriers along the optical spectrum.

Thus, the photocurrent out from the PD is

$$I_{\mathrm{PD}}(\omega) = \frac{1}{2\pi}\int_0^{+\infty} E_{\mathrm{out}}(\Omega)E_{\mathrm{out}}^{*}(\Omega-\omega)\mathrm{d}\Omega. \tag{8}$$

Comparing this to the Fourier transform of the input RF signal, the MPF's transfer function can be calculated finally as

$$H(\omega) \propto B\left(\omega+\frac{\Delta\tau}{\theta_2}\right)e^{j\left(\theta_2\frac{\omega^2}{2}-\Omega_0\Delta\tau\right)} + B\left(\omega-\frac{\Delta\tau}{\theta_2}\right)e^{-j\left(\theta_2\frac{\omega^2}{2}-\Omega_0\Delta\tau\right)}. \tag{9}$$

In the above expression, $B(\omega)$ is defined as

$$B(\omega) = \frac{1}{2\pi}\int_0^{+\infty} N(\Omega)e^{-j\omega\theta_2(\Omega-\Omega_0)}\mathrm{d}\Omega, \tag{10}$$

where $N(\Omega)$ is the BOS power spectral density. Since $\theta_2(\Omega-\Omega_0)$ in Eq. (10) is a time variant, this integral can be taken as a Fourier transform from the optical spectrum to the microwave frequency. Taking $B(\omega)$ as a baseband response, the $H(\omega)$ thus represents a transfer function of a single-bandpass filter centered at $\omega = \Delta\tau/\theta_2$, with the passband shape a scaled version of the Fourier transform of the BOS.

Figure 3 illustrates the mapping process from the optical spectrum to the RF domain caused by the transmission in the length of the DCF. As mentioned above, by directly beating the optical field before the DCF, each component of the original electrical slicing response would simultaneously occur at the time t_0, which consequently results in just a baseband response. After being dispersed by the DCF, a linear changed time delay is imposed along the optical spectrum. The red line in Fig. 3 obviously denotes that the slicing is extended consequently along the time axis. Applying this optical signal to a PD for square-law detection, the generated time-domain response is a truncated sinusoidal function with a FIR time duration of Δt, which starts at t_1 after the transmission in the DCF. Based on the Fourier transform theory, the frequency transmission function of the system is thus a bandpass filter. As the Δt of the truncated sinusoid response is related to the dispersed result of the BOS, the RF bandwidth should be reciprocal to the optical spectrum width of the BOS. By tuning the optical spectrum width of the BOS, the passband bandwidth of the MPF could also be continuously changed. Since the shape of the proposed MPF is related to the Fourier transform of the optical spectrum of the BOS, the shape of the MPF is reconfigurable by preprogramming the optical spectrum of the BOS using a wave shaper [14]. For example, this system can be used to generate the MPF with rectangular shape by programming the BOS in a sinc function manner with a user-defined phase in different taps, as demonstrated in [15,16].

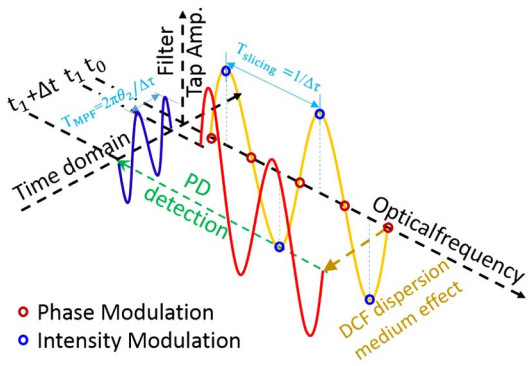

Fig. 3. Illustration of the optical frequency to time mapping effect caused by the DCF. Orange line: electrical slicing response before the DCF. Red line: linear time delay amount imposed onto the input optical field. Blue line: the final time domain impulse response of the MPF.

An experiment was carried out with the setup shown in Fig. 1. The polarization axes of the PDME, the PolM, and the Pol.1 and Pol.2 were set as described previously by adjusting the PCs. A linearly polarized BOS emitting with a span from 1556.65 to 1561.85 nm was sent into the PDME. After a delay in the PDME, the processed BOS was PC coupled into the PolM. The PolM was driven by a 20 GHz vector network analyzer (VNA, Agilent 8720D). The RF sweeping power of the VNA was constant at 10 dBm for small signal modulation. A PC was placed before the Pol.2 to adjust the input angle of the orthogonal polarized optical fields. After a 1130 m DCF, a PD with a bandwidth of 38 GHz and a conversion gain of 214 V/W was used to perform optical-to-electrical conversion. The output microwave current was fed back into the VNA. In addition, an optical spectrum analyzer (Advantest Q8384A) was employed to observe the optical spectra.

Figure 4(a) shows the measured optical spectrum of the BOS. A rectangular shape can be observed due to the inner TBPF with a flat top of 4.72 nm. Since the polarization of the Pol.2 was aligned with the PS1 and orthogonal with the PS2, we also measured each polarization state at the output of the Pol.2 while blocking the other one by turning on/off the optical switch in the PDME. As in Fig. 4(b), the PS1 was 35 dB higher than the PS2, which was ideal enough to apply in this system.

A mathematical simulation was carried out to verify the proposed filter. As shown in Fig. 5, when we took all the above parameters into Eq. (8) and chose the time delay equal to 14.3 ps, the calculated dashed response coincided well with the measured red curve, whose 3 dB passband bandwidth was 357 MHz centered at 4 GHz. The sidelobe suppression ratio was 13.4 dB, which was due to the rectangle like filtering window of the

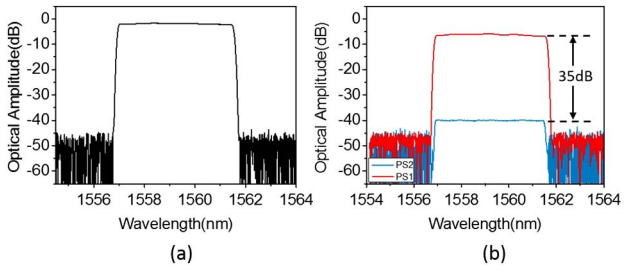

Fig. 4. (a) Optical spectrum of the BOS. (b) Result for each polarized state (PS1 and PS2) measured, respectively, at the output of Pol.2.

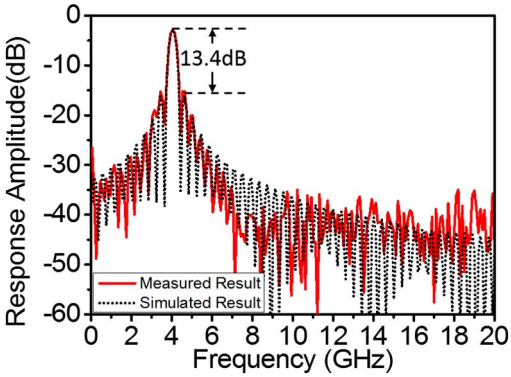

Fig. 5. Measured frequency response versus simulated response at 4 GHz.

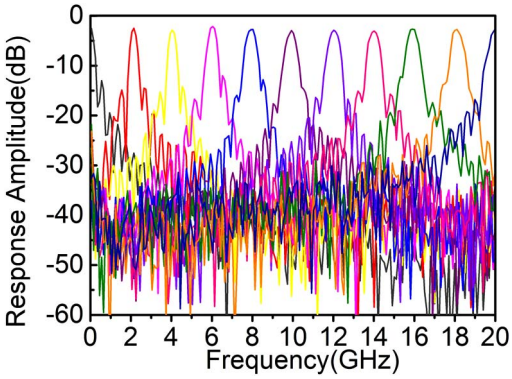

Fig. 6. Measured frequency responses of the proposed tunable MPF by adjusting the time delay through continuously tuning the VDL in the PDME.

TBPF after the ASE source. As the Fourier transform of a BOS with a rectangular shape is a sinc function in the RF domain (see Fig. 5), if the BOS with a Gaussian shape is applied to the proposed system, a single passband filter with a Gaussian-like shape can be achieved, which finally results in an improved out-of-band suppression ratio [12].

To test the tunability of the single-bandpass filter, the time delay difference between the two orthogonal polarized paths was tuned continuously from 0 to 71.4 ps in the PDME and the passband center moved from DC to 20 GHz. As the center frequency became higher, it also could be observed in Fig. 6 that the passband gradually broadened, which was caused by the third-order dispersion of the DCF. To fix this problem, low third-order dispersion devices, such as linear chirped FBGs, could be used in the future applications.

Finally, we adjusted the optical spectrum width of the BOS from 1 to 4 nm, as given in Fig. 7(b), which resulted in the changes of 3 dB bandwidth at 11.3 GHz from 1.343 to 0.447 GHz in Fig. 7(a). The ripples in the flat top of each optical spectrum in Fig. 7(b) resulted from the small interference between the PS1 and PS2 due to the fabrication precision of the PBS.

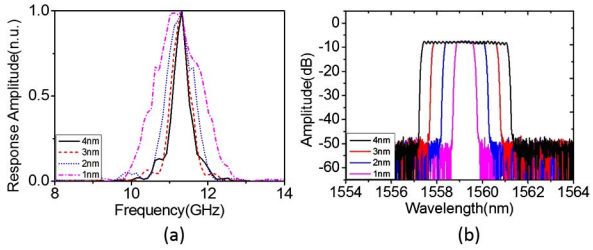

Fig. 7. (a) Frequency responses of the proposed MPF at different optical spectrum bandwidths from (b) 1 to 4 nm.

In conclusion, we theoretically and experimentally demonstrated a new scheme for photonic-based RF single-bandpass filter using a cascaded PolM, polarizer, PDME, and DCF. By inducing a tunable time delay between two polarized states, the center frequency of the passband could be continuously adjusted in a wide frequency range from DC to 20 GHz. By adjusting the optical spectrum width of the BOS, the 3 dB passband bandwidth was also shown to be tuned arbitrarily, which confirmed well the theoretical analysis. The proposed reconfigurable MPF has applications in high-speed photonic microwave signal processing systems to realize continuous single-frequency selection as well as improve the system's flexibility.

This research was supported by the National Natural Science Foundation of China under Grants Nos. 61108002, 61127018, 61106049, 61377071, 61177060, 61275031, 61177080, and 60820106004.

References

1. R. A. Minasian, IEEE Trans. Microwave Theory Tech. **54**, 832 (2006).
2. J. P. Yao, J. Lightwave Technol. **27**, 314 (2009).
3. J. Capmany, J. Mora, I. Gasulla, J. Sancho, J. Lloret, and S. Sales, J. Lightwave Technol. **31**, 571 (2013).
4. Y. Yan and J. Yao, Opt. Lett. **33**, 1756 (2008).
5. Y. Yu, E. Xu, J. Dong, L. Zhou, X. Li, and X. Zhang, Opt. Express, **18**, 25271 (2010).
6. T. Chen, X. Yi, T. X. H. Huang, and R. A. Minasian, Opt. Lett. **35**, 3934 (2010).
7. E. Hamidi, D. E. Leaird, and A. M. Weiner, IEEE Trans. Microwave Theory Tech. **58**, 3269 (2010).
8. W. Li, N. H. Zhu, and L. X. Wang, IEEE Photon. J. **3**, 462 (2011).
9. Y. M. Zhang and S. L. Pan, Opt. Lett. **38**, 802 (2013).
10. T. X. Huang, X. K. Yi, and R. A. Minasian, Opt. Express **19**, 6231 (2011).
11. X. X. Xue, X. P. Zheng, H. Y. Zhang, and B. K. Zhou, Opt. Express **19**, 18423 (2011).
12. L. W. Li, X. K. Yi, T. X. Huang, and R. A. Minasian, Opt. Lett. **38**, 1164 (2013).
13. S. L. Pan and Y. M. Zhang, Opt. Lett. **37**, 4483 (2012).
14. X. X. Xue, X. P. Zheng, H. Y. Zhang, and B. K. Zhou, J. Lightwave Technol. **31**, 2263 (2013).
15. X. X. Xue, X. P. Zheng, H. Y. Zhang, and B. K. Zhou, Opt. Express **20**, 26929 (2012).
16. M. Song, C. M. Long, R. Wu, D. Seo, D. E. Leaird, and A. M. Weiner, IEEE Photon. Technol. Lett. **23**, 1618 (2011).